RSC Advances

PAPER

Cite this: *RSC Adv.*, 2020, **10**, 11939

Crystal structure evolution of an energetic compound dihydroxylammonium 5,5′-bistetrazole-1,1′-diolate induced by solvents†

Xin Xu,[ab] Dong Chen,[a] Hongzhen Li,[a] Mi Yan,[a] Ying Xiong,[a] Haixia Zhao*[b] and Rong Xu*[a]

Received 7th February 2020
Accepted 15th March 2020

DOI: 10.1039/d0ra01182g

rsc.li/rsc-advances

Recently, energetic ionic salts have become a research hotspot due to their attractive properties, such as high density, high heat of formation, and environmental friendliness. Dihydroxylammonium 5,5′-bistetrazole-1,1′-diolate (**TKX-50**) is a typical nitrogen-rich energetic ionic salt, which has broad application prospects. However, the research on the stability and crystal structure evolution of **TKX-50** in different solvent systems is insufficient. Herein, we investigated the crystal structure transformations and searched for new solid forms of **TKX-50** under different conditions *via* a solvent induction method. The phase composition of all screened samples was analyzed by powder or single-crystal X-ray diffraction. Three new solid forms of $[NH_2(CH_3)_2^+][BTO^-]$, $[NH_2(CH_3CH_2)_2^+]_2[BTO^{2-}]$, $[NHOH(CH_3CCH_3)^+][BTO^-]$ H_2O were obtained from DMAC, DEF and AC/MT, respectively. Furthermore, the energetic properties were evaluated through EXPLO5.

Introduction

The solid form stability is one of the most important properties of explosives; different solid forms (such as solvates,[1] polymorphs[2] and salts[3]) will directly affect the safety, energy and storage life of weapons. In general, factors like solvents, temperature and pressure in crystallization can affect the crystalline solid forms of explosives due to the arisen changes in the structures of energetic molecules, and the transformed solid forms are irreversible in most cases. Among them, solvents act as the most important and influential role on the structure evolution in crystallization, but it has great unpredictability. During the crystallization process, some energetic compounds may react with the solvents to form solvates, salts or be induced to be a certain crystal polymorph. Unfortunately, these new solid forms hold serious drawbacks such as unstable structure, lower density and poor detonation performance, which have greatly limited their application. Up to now, the most used explosives' solid forms in the military are only as follows: α-RDX (hexahydro 1,3,5-trinitro-1,3,5-triazine),[4–7] β-HMX (1,3,5,7-tetranitro-1,3,5,7-azacyclo-octane),[8–10] ε-CL-20 (2,4,6,8-hexanitro-2,4,6,8,10,12-hexaazatetracyclododecane)[11,12] and α-FOX-7 (1,1-diamino-2,2-dinitroethylene).[13–15]

In recent years, energetic ionic salts (EISs) which consist of energetic cations and anions have been regarded as promising alternatives to molecular explosives such as RDX and HMX due to their good properties including high density, excellent safety and benign heat of formation.[16–24] However, it is worth noting that during the structural evolution of EISs induced by solvents, phase dissociation is an easily overlooked but important phenomenon compared to the possible polymorphs or solvent compounds. In phase dissociation, the primary multicomponent compound tend to dissociate to its unitary part, which can bring huge risks to explosives. In previous work, Li's[25] group has verified the phase dissociation phenomenon of energetic ionic salt carbonic dihydrazidinium bis [3-(5-nitroimino-1,2,4-triazolate)] (CBNT) for the first time. However, there is few study on the solid form transformations of high energy explosives especially for EISs for now, in which the cause and rule of series phenomenon are still unclear.[26] In order to further understand the physicochemical reliability of EISs, it is necessary to investigate their structure evolution and find the final solid forms in solvents induced crystallization process.

The energetic ionic salt dihydroxylammonium 5,5′-bistetrazole-1,1′-diolate (**TKX-50**) was first reported by Klapötke and coworkers[27] in 2012. Then, extensive attention has pointed to its excellent properties such as high density of 1.918 g cm^{-3}, high detonation velocity and pressure of 9698 ms^{-1} and 42.4 GPa, which showed great advantages and application prospects in the field of propellants. However, to the best of our knowledge, the previous research on **TKX-50** was mainly focused on the

[a]Institute of Chemical Materials, China Academy of Engineering Physics, Mianyang, 621900, China. E-mail: xurwjy@caep.cn

[b]College of Environment and Safety Engineering, North University of China, Taiyuan, 030051, China. E-mail: zhhx@nuc.edu.cn

† Electronic supplementary information (ESI) available. CCDC 1978629, 1978631 and 1978633. For ESI and crystallographic data in CIF or other electronic format see DOI: 10.1039/d0ra01182g

analysis[28,29] of synthetic methods and performance.[30–34] In 2009, Li *et al.*[35] found that **TKX-50** remains stable in DMSO, deionized water, ethyl acetate, acetonitrile, methanol, ethanol, petroleum ether and hexane. It is remarkable that **TKX-50** can react with DMF in different ways under different conditions, such as a wide temperature range from 25 °C to 150 °C. The products in reactions between **TKX-50** and DMF are dimethylammonium 5,5′-bistetrazole-1-hydroxy-1′-oxygen (**DMA-BTO**), dimethylamine 5,5′-bistetrazole-1,1′-diolate (**2DMA-BTO**) and diammonium 5,5′-bistetrazole-1,1′-diolate (**ABTOX**). However, this work only studied the structural transformation of **TKX-50** in limited pure solvents, and the result in binary solvent systems is unknown.

In this work, four different crystallization methods were used to study the crystal structure evolution of **TKX-50** in eight different solvent systems. Four powder samples and three single crystal structures were obtained through experiments. On the basis of previous work, we performed further crystallization experiments on DMF homologs including DMAC and DEF solvents, and found that the single crystal obtained from DMAC has the same crystal structure as obtained from DMF. An interesting experimental phenomenon is that although **TKX-50** can stably exist in pure solvent of acetone or methanol, a reaction occurred in their mixed solvent system. Moreover, the thermal and energy properties (standard molar enthalpy of formation, detonation velocity, and detonation pressure) of these new compounds were studied in detail.

Experimental

Solid form screening

The solubility of **TKX-50** in common solvents was tested, including: dimethyl sulfoxide (DMSO), distilled water (H_2O), *N*,*N*-diethyl methylformamide (DEF), *N*,*N*-dimethylacetamide (DMAC), *N*-methyl-2-pyrrolidone (NMP), 1,4-butyrolactone (BL), ethyl acetate ester (EA) and acetone (AC)/methyl alcohol (MT). The experimental process was as follows: added a certain amount of **TKX-50** to distilled water in a three-necked flask, stirred at room temperature, finally filtered and calculated the solubility of **TKX-50** in distilled water. Similarly, the solubility of **TKX-50** in the remaining solvents was listed in the Table 1. Solvents with the solubility above 0.01 g/100 mL were continued to be screened in solid form.

Seven solvents with the solubility higher than 0.01 g/100 mL were selected to screen possible **TKX-50** solids by screening solutions in the literature.[36] Added a certain amount of **TKX-50** to a three-necked flask with distilled water, stirred and heated until **TKX-50** completely dissolved and saturated. The resulting solution was evenly divided into four portions for processing in different ways. The first solution was quickly cooled to 0 °C by placing it in ice water and kept for 1 hour. The second solution was slowly cooled to room temperature in a ventilated place. The third part was covered with perforated plastic wrap and allowed to evaporate slowly. The fourth part was quickly evaporated using an air pump. Finally, the obtained precipitates were filtered, washed and dried.

Single crystal X-ray diffraction (SC-XRD)

Suitable crystals were chosen and placed in a Rigaku supernova Single X-ray Diffractometer area detector using graphite monochromated Mo Kα radiation ($\lambda = 0.71073$ Å) at 298(2) K. Their structures were solved by direct methods and successive Fourier difference syntheses using the SHELXTL software suite30. Hydrogen atoms attached to oxygen were placed from difference Fourier maps and were refined using riding model. Data collection parameters and refinement statistics were listed in Table S1.†

Powder X-ray diffraction (PXRD)

Powder X-ray diffraction patterns were recorded with the Cu Kα radiation ($\lambda = 1.54056$ Å). The current and voltage were set at 30 mA and 40 kV, respectively. The data were collected over the range from 5°to 50° with a step size of 0.02°.

Differential scanning calorimetry (DSC) and thermogravimetric (TG) analysis

DSC and TG analysis measurements were performed with a METTLER TOLEDO TGA/DSC2 calorimeter at a scan rate of 10 °C min^{-1} under nitrogen atmosphere of 20 mL min^{-1}.

Results and discussion

Solid form screening

In this paper, four different crystallization methods including quick cooling, slow cooling, quick evaporation, and slow evaporation were used to conduct screening experiments on the precipitation of **TKX-50**. The results were shown in Table 2.

According to Table 2, different crystallization methods and solvent systems had a large effect on the solid form of **TKX-50**. In our experiment, five solid samples were obtained, and we analyzed three structures among them including $DMAC_C$ ($[NH_2(CH_3)_2^+][BTO^-]$), DEF_C ($[NH_2(CH_3CH_2)_2^+]_2[BTO^{2-}]$), and AC/MT_C ($[NHOH(CH_3CCH_3)^+][BTO^-]\cdot H_2O$). The structure is shown in Fig. 1. As shown in Fig. 2, the PXRD patterns indicated that the solid samples obtained from different solvents had

Table 1 The solubility of TKX-50 in common solvents at 25 °C

Solubility	>0.5 g/100 mL	0.06 g/100 mL–0.5 g/100 mL	0.01 g/100 mL–0.06 g/100 mL	<0.01 g/100 mL
Solvent	DMSO	Water	DEF, DMAC, NMP, BL, AC/MT	EA

Table 2 The screening results for **TKX-50** in solution[a]

Solvent	Quick cooling	Slow cooling	Quick evaporation	Slow evaporation
DMSO	—	$DMSO_P$	—	$DMSO_P$
H_2O	H_2O_P	H_2O_P	H_2O_P	H_2O_P
DMAC	—	—	$DMAC_C$ (1)	—
DEF	—	—	DEF_C (2)	—
NMP	NMP_P	NMP_P	NMP_P	NMP_P
BL	BL_P	BL_P	BL_P	BL_P
AC/MT	—	—	—	AC/MT_C (3)

[a] —: no crystalline compound obtained, *P: powder, *C: single crystal.

different crystal structures, which due to the forming of new compounds that **TKX-50** crystallized in different solvents. For the DMAC solvent, the diffraction pattern of the obtained compound was completely different from the **TKX-50** raw material, and we define the product as **DMA-BTO**. However, single crystal diffraction indicated that the product obtained from the DMAC solvent had the same crystal structure as the product obtained from the DMF solvent. In addition, the product obtained from the DEF solvent which PXRD spectrum observed some new sharp peaks in the 2θ range of 5–10°and 15–

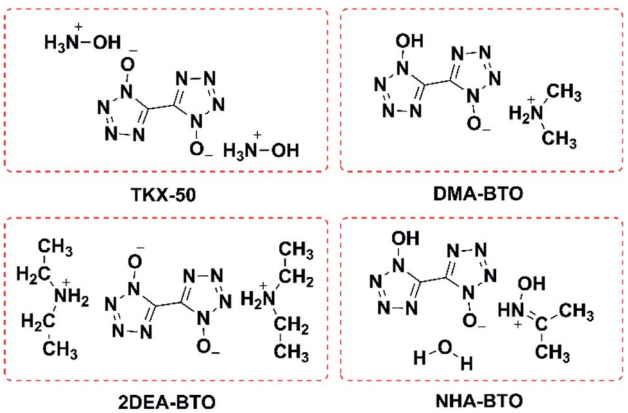

Fig. 1 The molecular structure of TKX-50, DMA-BTO, 2DEA-BTO and NHA-BTO.

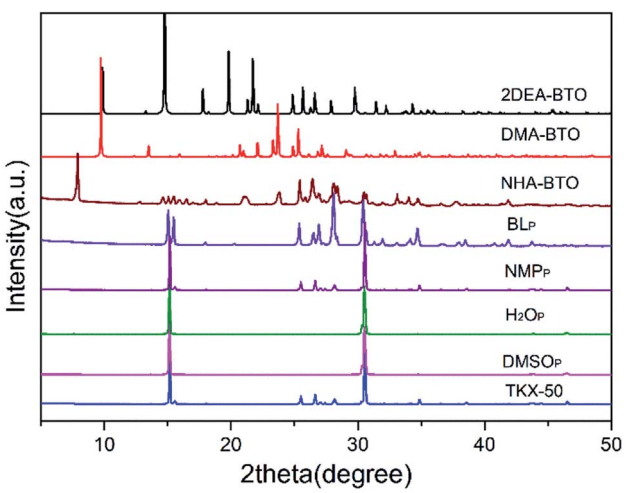

Fig. 2 Powder diffraction patterns of TKX-50 and the results by experiment.

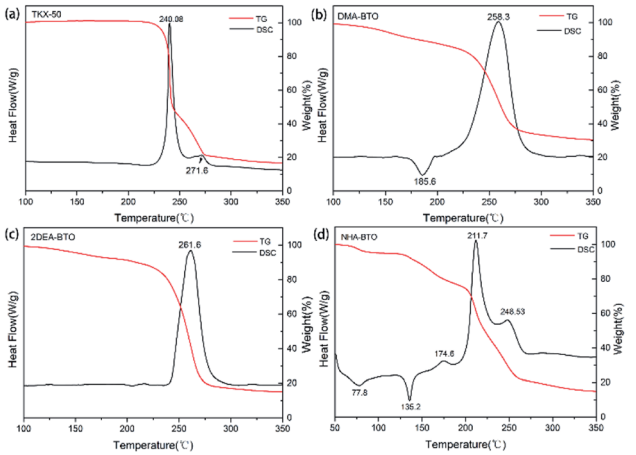

Fig. 3 TG-DSC curves, (a) TKX-50; (b) DMA-BTO; (c) 2DEA-BTO; (d) NHA-BTO.

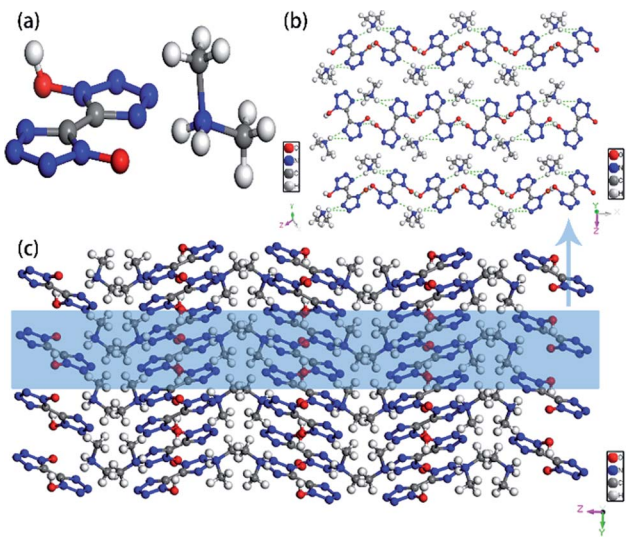

Fig. 4 (a) The asymmetric unit of DMA-BTO; (b) the layer structure contained in DMA-BTO; (c) the 3D extended structure of DMA-BTO.

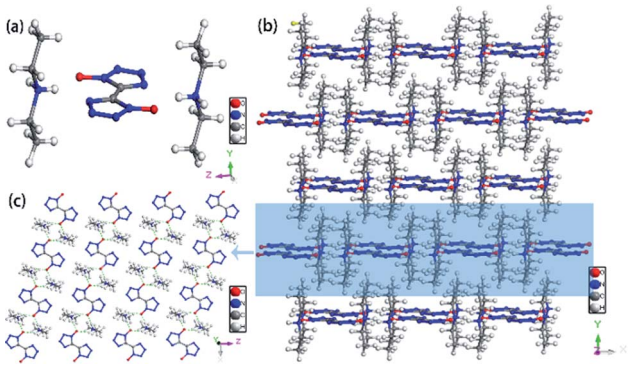

Fig. 5 (a) The crystal structure of 2DEA-BTO; (b) the layer structure contained in 2DEA-BTO; (c) the 3D extended structure of 2DEA-BTO.

25°was defined as 2DEA-BTO. The product obtained in the mixed solvent of acetone/methanol was defined as **NHA-BTO**, which was also with the different diffraction pattern from that of the raw material. In short, the diffraction peaks of the solids obtained in DMSO, H_2O, NMP, and BL were coincided with that of the raw material **TKX-50**, which indicated that the above five solvents could be used as solvents for recrystallization and process of **TKX-50**. In the studied solvent systems DEF, DMAC and mixed solvent of acetone/methyl alcohol, the crystal structure of **TKX-50** may be dissociated and formed other new compounds, which may destroy its original stability, safety and performance. Therefore, during the recrystallization, synthesis and storage of **TKX-50**, special care should be taken to avoid selecting these solvents.

An important index for evaluating high-energy materials was thermal stability, the thermal properties directly affect their safety performance and applications. Therefore, the thermal properties of the raw materials **TKX-50**, **DMA-BTO**, **2DEA-BTO** and **NHA-BTO** compounds were investigated *via* TG-DSC and the result curves were showed in Fig. 3. In general, the thermal

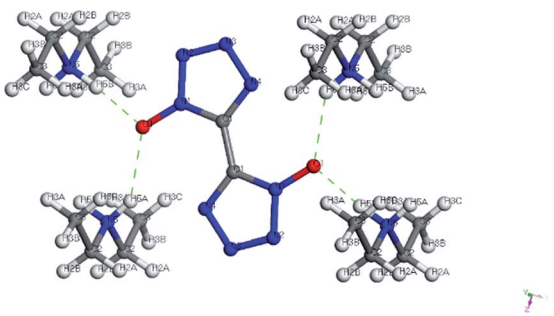

Fig. 6 The hydrogen bonds of the product 2DEA-BTO.

Table 3 Hydrogen bonds for 2DEA-BTO

D–H···A	*d*(D–H)	*d*(H···A)	*d*(D···A)	∠(DHA)
N(5)–H(5B)···O(1)	0.974	1.773	2.745	175.144
N(5)–H(5A)···O(1)	0.893	2.092	2.838	140.438

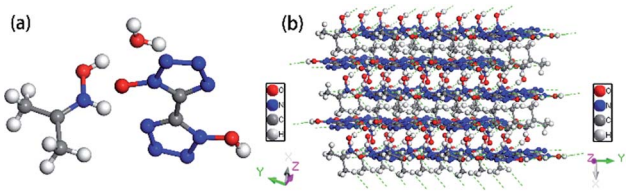

Fig. 7 (a) The asymmetric unit of NHA-BTO; (b) the layer structure contained in NHA-BTO.

behavior of the new compounds were significantly different from that of the raw materials. It could be seen from the curves that **TKX-50** showed distributed decomposition with two exothermic peaks, the main exothermic decomposition temperature peak was at 240.3 °C. For compound **DMA-BTO**, the main decomposition temperature was at 258.3 °C, there was also an endothermic peak at 185.6 °C and with 20% mass loss in the TG curve. We suspected that the escape of the internal solvent of the compound was not a simple solvent volatilization, causing higher temperature than the boiling point of DMAC solvent. The product **2DEA-BTO** had only one clear exothermic peak at 261.6 °C, which was about 20 °C higher than the decomposition temperature of the raw materials, indicating that the new compound showed excellent thermal stability. Meanwhile, the TG curve was decreased without obvious endothermic peaks, which indicated that the substance had sublimation properties. For the product **NHA-BTO**, the

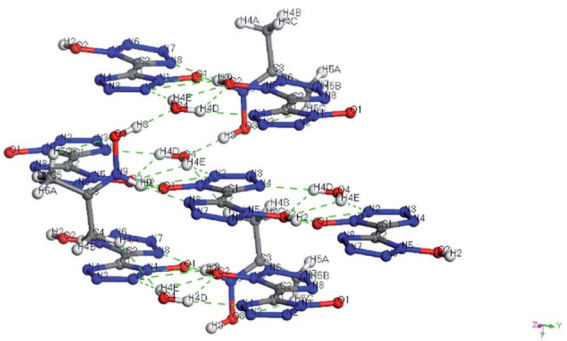

Fig. 8 The hydrogen bonds of the product NHA-BTO.

Table 4 Hydrogen bonds for 2DEA-BTO

D–H···A	*d*(D–H)	*d*(H···A)	*d*(D···A)	∠(DHA)
O(2)–H(2)···O(1)#1	0.946(18)	1.481(19)	2.4248(18)	175(3)
O(2)–H(2)···N(1)#1	0.946(18)	2.33(2)	3.1371(18)	143(3)
O(2)–H(2)···N(2)#1	0.946(18)	2.62(3)	3.112(2)	113(2)
C(4)–H(4A)···O(4)#2	0.99(3)	2.63(3)	3.448(3)	140(2)
N(9)–H(9)···O(1)	0.93(3)	2.47(3)	2.989(2)	115.6(19)
N(9)–H(9)···N(8)	0.93(3)	1.90(3)	2.795(2)	162(2)
O(3)–H(3)···O(4)	0.870(17)	1.653(18)	2.523(2)	178(3)
O(4)–H(4D)···N(4)#3	0.88(3)	2.00(3)	2.881(2)	175(3)
O(4)–H(4E)···O(2)#3	0.88(4)	2.42(3)	2.910(2)	116(3)
O(4)–H(4E)···N(2)#4	0.88(4)	2.16(4)	2.994(2)	158(3)

Table 5 Energetic properties of TKX-50 and compounds 1 to 3

Compound	ρ^a (g cm^{-3})	$T_d{}^b$ (K) °C	$\Delta_f H_m^{\theta\,c}$ (kJ mol^{-1})	P^d (GPa)	D^e (m s^{-1})
TKX-50	1.918	293	446.6	42.4	9698
DMA-BTO	1.529	293	711.8	23.7	8358.1
2DEA-BTO	1.172	293	548.4	13.6	7135.6
NHA-BTO	1.560	293	690.2	21.4	7863.5

[a] Density measured by gas pycnometer for **TKX-50** (25 °C) and SXRD for three new compounds. [b] Decomposition temperature. [c] Molar enthalpy of formation obtained by calculation. [d] Detonation pressure (calculated with EXPLO5 v6.02). [e] Detonation velocity (calculated with EXPLO 5 v6.02).

appearance of two endothermic peaks was mainly due to the evaporation of solvent methanol at 77.8 °C and the loss of crystalline water at 135.2 °C. More, the first decomposition peak of **NHA-BTO** was at 174.6 °C, also a clear exothermic peak appeared at 211.7 °C. At the same time, the thermal stabilities of the other five powder samples obtained during the screening were tested, and the results showed that their thermal behaviors were almost consistent with the raw material **TKX-50**.

Crystal structure

Colorless crystal of **DMA-BTO** ($[NH_2(CH_3)_2{}^+][BTO^-]$) was a product obtained by recrystallization from DMAC solution, which was crystallized in orthorhombic *Pbca* space group and with the density of 1.529 g cm^{-3}. This structure had been reported by Li *et al.*[35] but we crystallized the same crystal structure in different solvents DMAC, and analyzed the crystal structure here briefly. There was a BTO^- anion and a DMA^+ cation in the asymmetric unit of **DMA-BTO** (Fig. 4a). The anions and cations were connected by hydrogen bonds to form the one-dimensional chains like structures (Fig. 4b), these hydrogen bonds are as follow: N–H···N, N–H···O, O–H···O and O–H···N. The adjacent chains were arranged together to form a 2D layer, and then the layer structures were packed to form the 3D extended structure of **DMA-BTO** (Fig. 4c).

Colorless crystal of **2DEA-BTO** ($[NH_2(CH_3CH_2)_2{}^+]_2[BTO^{2-}]$) was a product obtained by recrystallization from DEF solution, which was crystallized in monoclinic *C*2/*m* and with the density of 1.172 g cm^{-3}. There was one BTO^{2-}anion and two DEA^+ cations in the asymmetric unit of **2DEA-BTO** (Fig. 5a). Each BTO^{2-} anion was interacted with two adjacent DEA^+ anions to form a linear structure running along *X*-axis direction *via* hydrogen bonds of NH···O, the adjacent linear structures were arranged with each other to form layer structures (Fig. 5b). In order to better understand the substance, we performed a detailed analysis of hydrogen bonding shown in Fig. 6. The type of hydrogen bonding was N–H···O and the bond length was in the range of 2.745–2.838 Å, which were listed in Table 3. Finally, the layer structures were packed into a 3D extended structure of $[NH_2(CH_3CH_2)_2{}^+]_2[BTO^{2-}]$ (Fig. 5c).

Colorless crystal of **NHA-BTO** ($[NHOH(CH_3CCH_3)^+][BTO^-]\cdot H_2O$) was the product obtained by recrystallization from AC/MT mixed solution, which belonged to triclinic $P\bar{1}$ space group and with the density of 1.560 g cm^{-3}. The asymmetric unit of **NHA-BTO** contained a BTO^- anion, a $NHOH(CH_3CCH_3)^+$ cation, and a water molecule shown in Fig. 7a. The 3D structure of **NHA-BTO** (Fig. 7b) was within five types of hydrogen bonds. To be specific, each BTO^- anion was interacted with adjacent BTO^- anions *via* hydrogen bonds of O–H···N, in which the bond length was in the range of 3.112–3.137 Å. Each BTO^- anion was interacted with adjacent $NHOH(CH_3CCH_3)^+$ cation *via* hydrogen bonds of N–H···O and N–H···N, the bond lengths of N–H···O, N–H···N were 2.989 Å and 2.795 Å, respectively. Each BTO^- anion was interacted with two water molecule *via* the hydrogen bonds of O–H···N and O–H···O, the hydrogen bond lengths of O–H···N, O–H···O were in the range of 2.881–2.994 Å and 2.910 Å, respectively. Moreover, each $NHOH(CH_3CCH_3)^+$ anion was interacted with a water molecule *via* hydrogen bonds of O–H···O, the bond length was 2.523 Å. Similarly, the hydrogen bonds contained in the structure were summarized in Fig. 8 and Table 4.

Energetic properties

Detonation velocity (*D*) and detonation pressure (*P*) are important parameters for evaluating the explosion characteristics of high-energy materials. In order to verify the energy characteristics of the obtained crystals, the standard molar enthalpy of formation ($\Delta_f H_m^{\theta}$) of compounds was calculated *via* Energetic Materials Studio 1.0 (ESI†), and the detonation velocity (*D*) and detonation pressure (*P*) of the new compounds were further calculated by EXPLO5 version 6.02 (ref. 37) and the results were shown in Table 5. Compared with the detonation velocity (9698 m s^{-1}) and detonation pressure (42.4 GPa) of the raw material **TKX-50**, the detonation properties of three obtained compounds in this work were significantly reduced. Among these three compounds, compound **DMA-BTO** showed the highest detonation performance with the detonation velocity and detonation pressure values of 8358.1 m s^{-1} and 23.7 GPa, respectively. The **2DEA-BTO** with the detonation velocity and detonation pressure values of 7135.6 m s^{-1} and 13.6 GPa, also the **NHA-BTO** with the detonation velocity and detonation pressure values of 7863.5 m s^{-1} and 21.4 GPa, respectively. In short, these new compounds have significantly destroyed the excellent performance of **TKX-50**. Although energetic ionic salts have been widely studied in the field of energetic materials and have many advantages, we also need to consider their solid form stability in the application of weapons.

Conclusions

In summary, we applied four crystallization methods to study the effect of different solvents on the structural evolution of

energetic compound **TKX-50**. Several powder samples and three single crystal structures have been successfully screened. Among them, the compound $[NH_2(CH_3)_2^+][BTO^-]$ was obtained by crystallization in DMAC, the compound $[NH_2(CH_3CH_2)_2^+]_2[BTO^{2-}]$ was obtained in DEF, and the compound $[NHOH(CH_3CCH_3)^+][BTO^-]\cdot H_2O$ was obtained in acetone/methyl alcohol mixed solvent. This work further demonstrates the possible evolution of **TKX-50** during the induction of different solvent systems. Results showed that the use of three solvents (acetone/methyl alcohol, DMAC and DEF) would change the original structure of **TKX-50**. More important, the results obtained here could increase our knowledge of **TKX-50** and reduce the security risks during future synthesis and storage.

Conflicts of interest

There are no conflicts to declare.

Acknowledgements

This work was supported by the National Nature Science Foundation of China (no. 21875231). We appreciate Prof. Chaoyang Zhang's group for their generous assistance in terms of enthalpy calculations.

References

1 U. J. Griesser, *Polymorphism in the pharmaceutical industry*, 2006, pp. 211–233.
2 D. Giron, *Thermochim. Acta*, 1995, **248**, 1–59.
3 S. L. Morissette, Ö. Almarsson, M. L. Peterson, J. F. Remenar, M. J. Read, A. V. Lemmo, S. Ellis, M. J. Cima and C. R. Gardner, *Adv. Drug Delivery Rev.*, 2004, **56**, 275–300.
4 J. H. Ter Horst, R. M. Geertman, A. E. Van der Heijden and G. M. Van Rosmalen, *J. Cryst. Growth*, 1999, **198**, 773–779.
5 D. I. A. Millar, I. D. H. Oswald, D. J. Francis, W. G. Marshall, C. R. Pulham and A. S. Cumming, *Chem. Commun.*, 2009, **5**, 562–564.
6 R. J. Karpowicz, S. T. Sergio and T. B. Brill, *Ind. Eng. Chem. Prod. Res. Dev.*, 1983, **22**, 363–365.
7 C. S. Choi and E. Prince, *Acta Crystallogr., Sect. B: Struct. Sci., Cryst. Eng. Mater.*, 1972, **28**, 2857–2862.
8 Y. Bayat, M. Eghdamtalab and V. Zeynali, *J. Energ. Mater.*, 2010, **28**, 273–284.
9 H. Kröber and U. Teipel, *Propellants, Explos., Pyrotech.*, 2008, **33**, 33–36.
10 P. Soni, C. Sarkar, R. Tewari and T. D. Sharma, *J. Energ. Mater.*, 2011, **29**, 261–279.
11 G. Liu, R. Gou, H. Li and C. Y. Zhang, *Cryst. Growth Des.*, 2018, **18**, 4174–4186.
12 J. C. Bennion, N. Chowdhury, J. W. Kampf and A. J. Matzger, *Angew. Chem., Int. Ed. Engl.*, 2016, **128**, 13312–13315.
13 U. Bemm and H. Östmark, *Acta Crystallogr., Sect. C: Cryst. Struct. Commun.*, 1998, **54**, 1997–1999.
14 J. Evers, T. M. Klapötke, P. Mayer, G. Oehlinger, J. Welch and K. Inorg, *Chem*, 2006, **45**, 4996–5007.
15 M. J. Crawford, J. Evers, M. Göbel, T. M. Klapötke, P. Mayer, G. Oehlinger and J. M. Welch, *Propellants, Explos., Pyrotech.*, 2007, **32**, 478–495.
16 R. P. Singh, R. D. Verma, D. T. Meshri and J. M. Shreeve, *Angew. Chem., Int. Ed.*, 2006, **45**, 3584–3601.
17 P. He, J. G. Zhang, X. Yin, J. T. Wu, L. Wu, Z. N. Zhou and T. L. Zhang, *Chem.–Eur. J.*, 2016, **22**, 7670–7685.
18 T. M. Klapotke, P. Mayer, A. Schulz and J. J. Weigand, *J. Am. Chem. Soc.*, 2005, **127**, 2032–2033.
19 Z. Zeng, H. X. Gao, B. Twamley and J. M. Shreeve, *J. Mater. Chem.*, 2007, **17**, 3819–3826.
20 M. J. Crawford, T. M. Klapotke, F. A. Martin, C. M. Sabate and M. Rusan, *Chem.–Eur. J.*, 2011, **17**, 1683–1695.
21 C. F. Ye, J. C. Xiao, T. Brendan and J. M. Shreeve, *Chem. Commun.*, 2005, **21**, 2750–2752.
22 T. M. Klapotke, C. M. Sabate and M. Rasp, *J. Mater. Chem.*, 2009, **19**, 2240–2252.
23 Y. HyukJoo and J. M. Shreeve, *Angew. Chem., Int. Ed.*, 2010, **49**, 7320–7323.
24 H. Xue and J. M. Shreeve, *Adv. Mater.*, 2005, **17**, 2142–2146.
25 J. R. Ren, D. Chen, G. R. Liu, K. C. Wang, G. J. Fan, Y. W. Yu, C. Y. Zhang and H. Z. Li, *CrystEngComm*, 2020, **22**, 593–601.
26 O. D. Putra, T. Yoshida, D. Umeda, M. Gunji, H. Uekusa and E. Yonemochi, *Cryst. Growth Des.*, 2016, **16**, 5223–5229.
27 N. Fischer, D. Fischer, T. M. Klapötke, D. J. Piercey and J. Stierstorfer, *J. Mater. Chem.*, 2012, **22**, 20418–20422.
28 P. W. Ju, F. Y. Ling, Y. F. Gu and J. Luo, *J. Energ. Mater.*, 2015, **9**, 887–891.
29 F. Bi, C. Xiao, C. Xu, Z. Ge, B. Wang, X. Fan and W. Wang, *J. Energ. Mater.*, 2014, **22**, 272–273.
30 N. Fischer, T. M. Klapötke, M. Reymann and J. Stierstorfer, *Eur. J. Inorg. Chem.*, 2013, **12**, 2167–2180.
31 H. Huang, Y. Shi and J. Yang, *J. Therm. Anal. Calorim.*, 2015, **121**, 705–709.
32 L. Xiao, F. Zhao, Y. Luo, N. Li, H. X. Gao, Q. Y. Xue, Z. Cui and Z. R. Hu, *J. Therm. Anal. Calorim.*, 2016, **1**, 653–657.
33 H. Niu, S. Chen, S. Jin, L. Li, B. Jiang, Z. Jiang, J. Ji and Q. Shu, *J. Therm. Anal. Calorim.*, 2016, **2**, 473–480.
34 N. V. Muravyev, K. A. Monogarov and A. F. Asachenko, *Phys. Chem. Chem. Phys.*, 2016, **1**, 436–449.
35 J. Jia, J. Xu, X. Cao, S. Li, S. L. Huang, Y. Liu and J. S. Li, *Propellants, Explos., Pyrotech.*, 2019, **44**, 989–999.
36 V. Zvoníček, E. Skořepová, M. Dušek, M. Babor, P. Zvatora and M. Sooš, *Cryst. Growth Des.*, 2017, **17**, 3116–3127.
37 M. Sućeska, *EXPLO5 V6.02*, Brodarski Institute, Zagreb, Croatia, 2014.

